SCIENCE CHINA
Life Sciences

• RESEARCH PAPER •

March 2017 Vol.60 No.3: 264–270
doi: 10.1007/s11427-016-0183-1

Histone methyltransferase TXR1 is required for both H3 and H3.3 lysine 27 methylation in the well-known ciliated protist *Tetrahymena thermophila*

Xiaolu Zhao[1†], Yuanyuan Wang[1†], Yurui Wang[1†], Yifan Liu[2] & Shan Gao[1,3*]

[1]*Institute of Evolution & Marine Biodiversity, Ocean University of China, Qingdao 266003, China;*
[2]*Department of Pathology, University of Michigan, Ann Arbor MI 48109, USA;*
[3]*Laboratory for Marine Biology and Biotechnology, Qingdao National Laboratory for Marine Science and Technology, Qingdao 266003, China*

Received June 20, 2016; accepted August 16, 2016; published online October 17, 2016

DNA replication elongation is tightly controlled by histone-modifying enzymes. Our previous studies showed that the histone methytransferase TXR1 (*Tetrahymena Trithorax* related protein 1) specifically catalyzes H3K27 monomethylation and affects DNA replication elongation in *Tetrahymena thermophila*. In this study, we investigated whether TXR1 has a substrate preference to the canonical H3 over the replacement variant H3.3. We demonstrated by histone mutagenesis that K27Q mutation in H3.3 further aggravated the replication stress phenotype of K27Q mutation in canonical H3, supporting H3.3 as a physiologically relevant substrate of TXR1. This result is in apparent contrast to the strong preference for canonical H3 recently reported in *Arabidopsis* homologues ATXR5 and ATXR6, and further corroborates the role of TXR1 in DNA replication.

replication, histone, TXR1, *Tetrahymena*, substrate preference

Citation: Zhao, X., Wang, Y., Wang, Y., Liu, Y., and Gao, S. (2017). Histone methyltransferase TXR1 is required for both H3 and H3.3 lysine 27 methylation in the well-known ciliated protist *Tetrahymena thermophila*. Sci China Life Sci 60, 264–270. doi: 10.1007/s11427-016-0183-1

INTRODUCTION

DNA in eukaryotic cells is packed with histones to form nucleosome and higher-order structures (Beh et al., 2015; Kornberg and Thonmas, 1974). Each transaction of DNA (e.g. replication, transcription, repair) is affected by the epigenetic information carried by histone post-translational modifications (PTMs), as well as histone-modifying enzymes (Berger, 2002; Burman et al., 2015; Engelen et al., 2015; Felsenfeld and Groudine, 2003; Iizuka and Smith, 2003; Strahl and Allis, 2000). Our previous study revealed that the H3 lysine methyltransferase TXR1 (*Tetrahymena Trithorax* related protein 1) deposits mono-methylation on the lysine 27 residue of major H3, and knockout of TXR1 causes severe replication stress (Gao et al., 2013; Zhang et al., 2014). For example, there is accumulation of single-stranded DNA around replication origins and DNA repair pathways are extensively activated. Meanwhile, the *Arabidopsis* homologues of TXR1, ATXR5 and ATXR6, are reported to maintain the heterochromatin marker H3K27me1 during replication in plants. The *atxr5 atxr6* hypomorphic mutants showed reduced level of H3K27me1 and overreplication in heterochromatin regions, independent of DNA methylation and H3K9 methylation (Jacob et al., 2009, 2010).

Tetrahymena thermophila is a well-established ciliate model organism for molecular and cellular biology (Figure 1 and 2A–F) (Meyer and Chalker, 2007). Like other ciliates,

†Contributed equally to this work
*Corresponding author (email: shangao@ouc.edu.cn)

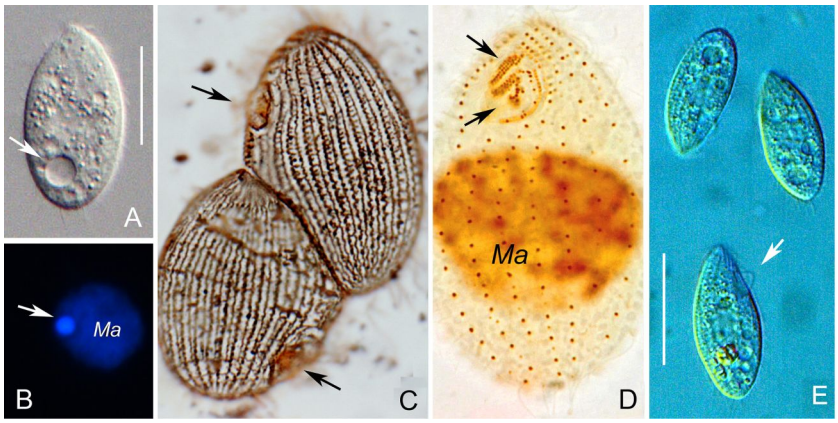

Figure 1 Morphology of *Tetrahymena thermophila*. A and E, Cells *in vivo*, arrow in A indicates the contractile vacuole while in E marks the paroral membrane. B, Macronucleus (Ma) and micronucleus (arrow). C, Silverline system, arrows indicate the buccal field. D, Infraciliature, arrows point the membranelles. Scale bar=20 μm.

Tetrahymena has two structurally and functionally differentiated nuclei, the macronucleus (MAC) and the micronucleus (MIC) (Chen et al., 2016; Gao et al., 2016; Karrer and VanNuland, 2002; Liu et al., 2016). The *Tetrahymena* histone H3 multigene family consists of three types of variant: major H3, quantitatively minor H3.3, and the centromere-specific CenH3. The minor H3.3, also called replacement H3, differs from the major H3 in several amino acids and functions in a distinct way. In animals and plants, major H3 was deposited only during replication by the histone chaperone CAF-1, while replacement histones H3.3 and H3.4 are inserted by other chaperones such as HIRA in a replication-independent (RI) way (Ray-Gallet et al., 2002; Tagami et al., 2004). In *Tetrahymena*, *HHT1* (TTHERM_00570560) and *HHT2* (TTHERM_00189180) encode the same major H3 protein**.** *HHT3* (TTHERM_00016170) encodes the minor variant H3.3, which differs from major H3 at 16 residues (Allis et al., 1980; Bannon et al., 1983; Thatcher et al., 1994). *HHT4* (TTHERM_00016200) encodes the minor variant H3.4, which differs from H3.3 by 5 amino acids and functions similarly to H3.3 (Cui et al., 2006). In contrast, *Tetrahymena* H3.3 and H3.4 can be deposited not only by the RI pathway, but also by the replication-coupled (RC) pathway (Cui et al., 2006). Moreover, it was documented that *Tetrahymena* and plant replacement H3 evolved independently (Thatcher and Gorovsky, 1994).

A recent study reports that ATXR5 and ATXR6 can selectively methylate the replication-dependent H3.1 but not the replication-independent H3.3 (Jacob et al., 2014). The authors inferred from the crystal structure that Ala31, which is very close to the methylation site K27 in H3.1 and conserved in plants and animals, plays a vital role in the substrate selection. H3.3 cannot be efficiently methylated because of a bulky threonine substitution at position 31 that inhibits substrate binding to ATXR5 and ATXR6 by steric clash. We therefore investigated whether TXR1, specific for H3 lysine 27 mono-methylation (H3K27me1) (Gao et al., 2013), also utilized the replacement variant H3.3. Using specialized strains and genetic manipulation, we demonstrated that lysine to glutamine mutation (K27Q) in H3.3 further aggravated the replication stress phenotype of cells with K27Q mutation in canonical H3, supporting H3.3 as a physiologically relevant substrate of TXR1 in *Tetrahymena*.

RESULTS AND DISCUSSION

Generating complete somatic replacement strains of *HHT2*-WT/*HHT3*-WT and *HHT2*-K27Q/*HHT3*-K27Q

HHT3-WT/ΔHHT4-chx and HHT3-K27Q/ΔHHT4-chx plasmid were transformed into HHT2-WT or HHT2-K27Q cells. In non-transformants, the flanking primers will generate a product of ~160 base pairs. In transformants where the drug-resistance cassette was inserted in the 3′ flanking region, no PCR product could be amplified from the macronucleus (MAC) DNA, only from the germ line micronucleus (MIC). It is empirically determined that the DNA ratio of MAC/MIC is about 16 (2^4). This ratio is calculated based on two facts: (i) most genes in MAC is between 45C (G1 phase) and 90C (G2 phase) (Woodard et al., 1972); (ii) MIC is essentially 4C with no apparent G1 phase (Cole and Sugai, 2012). As our primers were designed to amplify the deleted region (Figure 2), it requires 4 more cycles for transformants to obtain equal quantity of PCR products than WT control cells ((45+90)/2/4=16;16=2^4.) Therefore, transformed cells with a normalized Ct difference more than 4 ($\Delta C_t \geqslant 4$; relative to WT cells) are assumed to achieve complete replacement in MAC. Our QPCR analysis successfully selected HHT3-WT_ΔHHT4 transformants with $\Delta C_t \geqslant 4$ in the background of HHT2-WT, as HHT2-WT/HHT3-WT. It should be noted, however, MICs in HHT2-K27Q cells tend to be lost, even after several rounds of rejuvenation. Therefore, PCR products could only be amplified from MAC DNA. Cells with $\Delta C_t \geqslant 30$ or with no amplification were selected as complete replacement transformants of HHT2-K27Q/HHT3-

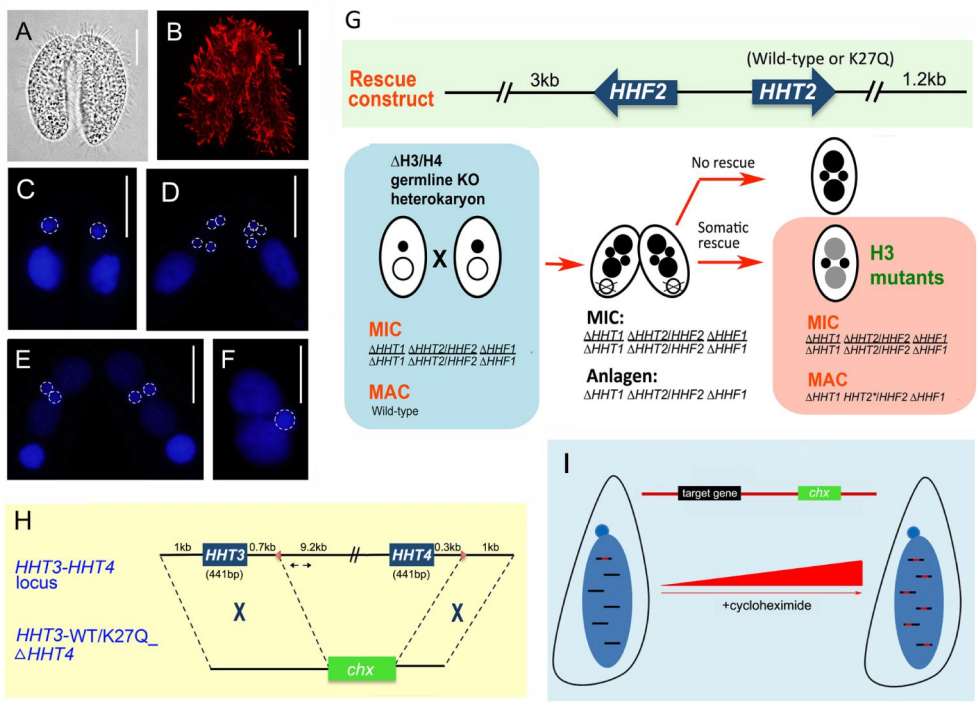

Figure 2 Generation of *HHT2*-WT/*HHT3*-WT and *HHT2*-K27Q/*HHT3*-K27Q strains. A–F. Cells in conjugation *in vivo* (A) and stained with anti-tubulin antibody (B), 4′,6-diamidino-2-phenylindole (DAPI) staining of cells in early (C), middle (D), late (E) and exconjugant (F) stages of conjugation; Dashed circles indicate micronucleus (MIC). G, Generation of *HHT2*-WT/K27Q cells, modified from (Liu et al., 2004). H, Schematics for the *HHT3-HHT4* endogenous locus and the locus in *HHT2*-WT/*HHT3*-WT and *HHT2*-K27Q/*HHT3*-K27Q cells. The *chx* cassette was inserted into the 3′ UTR of *HHT3*. The whole coding sequence (CDS) of *HHT4* was deleted. *HHT2*-WT/*HHT3*-WT and *HHT2*-K27Q/*HHT3*-K27Q cells were generated by transforming *HHT3*-WT/Δ*HHT4*-chx and *HHT3*-K27Q/Δ*HHT4*-chx plasmids into *HHT2*-WT/K27Q cells. Arrowheads indicate where *chx* cassette was inserted. Arrows indicate the primers used for quantitative PCR confirmation. I, Drug selection to generate the complete somatic replacement of *HHT2*-WT/*HHT3*-WT and *HHT2*-K27Q/*HHT3*-K27Q strains. Concentration of cycloheximide was doubled every other day for complete assortment of *HHT3* in MAC. Scale bar=10 μm.

K27Q (Table 1).

Both H3 and H3.3 are the physically relevant substrate of TXR1

Our previous study pinpointed TXR1-catalyzed H3K27me1 as the relevant modification that affects replication elongation (Gao et al., 2013). Surprisingly, site-directed mutagenesis on H3 K27 (*HHT2*-K27Q) can only partially mimic the phenotype of Δ*TXR1* cells. It has weak signal for the DNA damage marker, γH2A.X and the ssDNA indicator BrdU (non-denaturing). Only the most sensitive marker, ssDNA-binding protein RPA1, shows significantly stronger signal in G2 and amitosis (AM) phase than the wild-type counterpart. This strongly suggests that TXR1 may have other histone substrates or even non-histone substrates.

To determine whether H3.3 K27 is also the relevant substrate of TXR1, we engineered a double mutation strain in which K27Q mutation was introduced to both the major H3 and minor H3.3. The *HHT2*-K27Q mutation was previously introduced into macronucleus by rescuing the conjugation progenies of homozygous heterokaryon Δ*HHT1*/Δ*HHT2*/Δ*HHF1*/Δ*HHF2* (ΔH3/ΔH4) cells, the paromomycin resistance of which was conferred by the *neo2* cassette (Liu et al., 2004). The *HHT3*-K27Q mutation was introduced into the macronucleus of *HHT2*-K27Q rescue cells with the cycloheximide resistance conferred by the *chx* cassette. The neighboring *HHT4* (10 kb downstream of *HHT3*), whose encoded protein was shown to be functionally redundant to H3.3 (Cui et al., 2006), was deleted in the *HHT3* mutagenesis construct. Phenotypic analysis demonstrated that H3.3 K27Q further aggravated the replication stress phenotype of H3 K27Q, with more ssDNA accumulation demonstrated by the non-denaturing BrdU staining (Figure 3). In total 100 cells were counted for each type of cells. Respectively, ~20%, 30% and 50% of *HHT2*-WT/*HHT3*-WT, *HHT2*-K27Q/*HHT3*-WT and *HHT2*-K27Q/*HHT3*-K27Q cells have the indicated phenotypes. The phenotype was caused by the targeted mutation but not some unknown effects of genetic disruption, because the control cells (*HHT2*-WT/*HHT3*-WT) were not affected. Consistent with this, Δ*TXR1* cells showed dramatically reduced mono-methylation levels not only for H3 K27, but also for H3.3 K27 (Zhang et al., 2013), substantiating the involvement of H3.3 K27. Thus, for *Tetrahymena*, both H3 K27 and H3.3 K27 are the relevant substrate of TXR1.

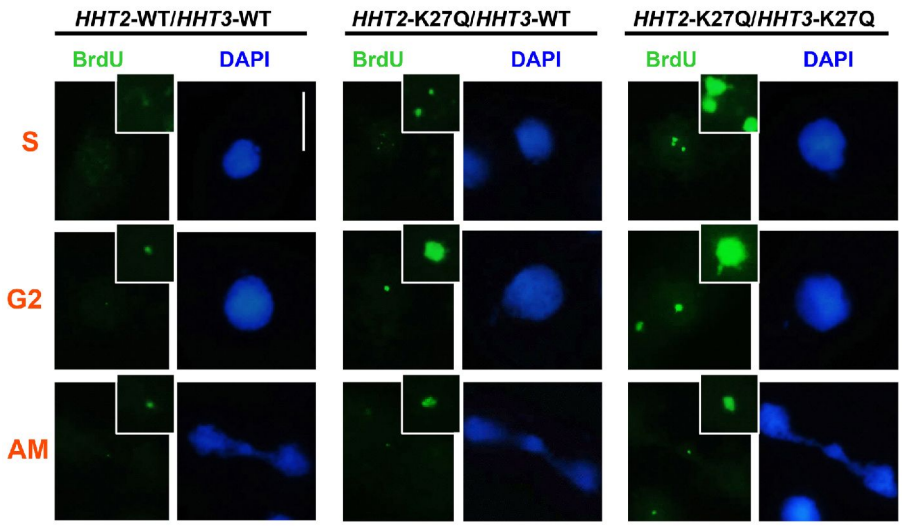

Figure 3 (Color online) Both major H3 and replacement variant H3.3 are physically relevant substrates of TXR1. H3.3 K27Q aggravates the phenotype of H3 K27Q. Cells were labeled with BrdU (0.1 mmol L^{-1}) overnight and log-phase growing cells were fixed for immunofluorescent staining. The anti-BrdU antibody incubation was performed without denaturation. S, S and early-G2 phase; G2, mid- and late-G2 phase; AM, amitosis; Scale bar=10 μm.

Table 1 QPCR data for validation of complete somatic replacement of *HHT2*-WT/*HHT3*-WT and *HHT2*-K27Q/*HHT3*-K27Q strains[a)]

Sample		Normalization by JMJ1	Average	Normalization by control
HHT2-WT/*HHT3*-WT	1	6.73	6.52	5.67
	2	6.31		
HHT2-K27Q/*HHT3*-K27Q	1	no amplification	∞	∞
	2	no amplification		
HHT2-WT*	1	1.02	0.85	0
	2	0.69		
HHT2-K27Q/*HHT3*-WT**	1	0.39	0.43	0
	2	0.47		

a) *, control to *HHT2*-WT/*HHT3*-WT. **, control to *HHT2*-K27Q/*HHT3*-K27Q.

Different substrate specificity between TXR1 and ATXR5/6

It was reported that the *Arabidopsis* homologues of TXR1, ATXR5 and ATXR6, could selectively methylate the replication-dependent H3.1 but not the replication-independent H3.3 (Jacob et al., 2014). The authors attributed this preference to the alanine to threonine substitution in H3.3 that inhibits its binding to ATXR5 and ATXR6. This is in apparent contrast to our result. Of note, *Tetrahymena* H3.3 has a valine (Val) at position 31 instead of a threonine (Figure 4A). Structurally, valine and threonine have similar shapes, though different polarity. There are also no other differences in neighboring residues around H3/H3.3 K27 that can account for the difference (Figure 4A). Therefore, we further examined the sequence difference between *Tetrahymena* TXR1 and *Arabidopsis* ATXR5/ATXR6. We found that a loop (L3) in ATXR5 comprising residues G363, Y364, E365, and E367, playing critical roles in differentiating H3 and H3.3, is not conserved in *Tetrahymena* TXR1, as well as homologues in other protozoa, mosses, and even many higher plants (Figure 4B). Functionally, *Tetrahymena* H3.3 as well as its orthologues in other eukaryotes can be deposited not only in the replication-independent pathway, but also in varying degree in the replication-coupled pathway (Ahmad and Henikoff, 2002; Cui et al., 2006). This raised the necessity for H3.3 K27 to be methylated by TXR1 during replication.

Based upon our histone mutagenesis as well as Mass Spectrometry results, we favor the hypothesis that selective methylation of H3.1 by *Arabidopsis* ATXR5/ATXR6 is not widely employed as a strategy to differentiate between the canonical histone H3 and conserved variant H3.3. In *Tetrahymena* as well as a diverse range of eukaryotes, TXR1 and its homologues can catalyze mono-methylation at K27 of any histone H3 (H3 and H3.3) deposited during replication, and through a mechanism yet to be elucidated, efficiently manage replication stress.

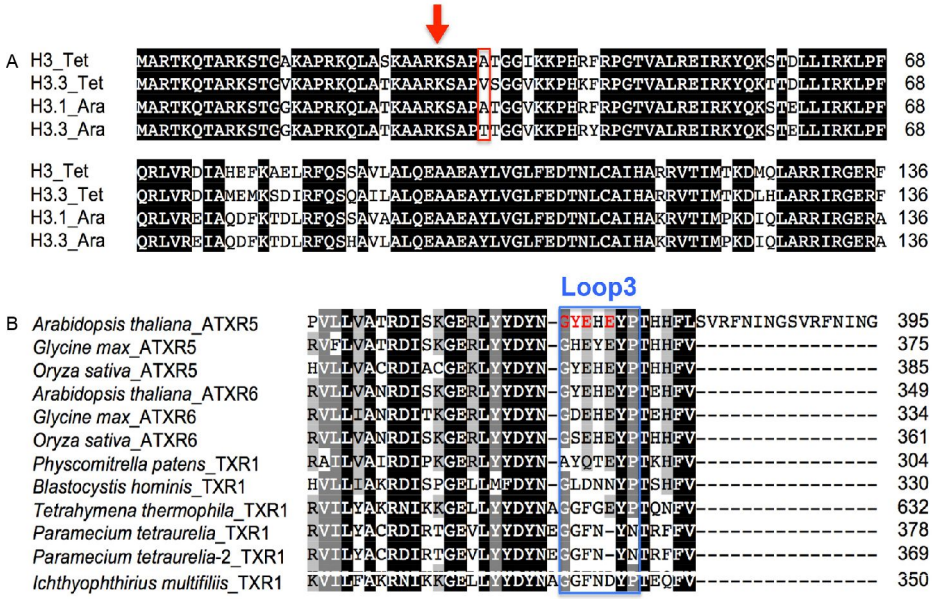

Figure 4 Comparison of H3 homologues and TXR1 homologues. A, Sequence alignment of *Tetrahymena thermophila* histone H3 (H3_Tet), H3.3 (H3.3_Tet), *Arabidopsis thaliana* histone H3 (H3_Ara), and H3.3 (H3.3_Ara). Identical amino acids are dark-shaded. Lysine 27 is marked by a red arrow. Residues at position 31 were circled with a red box. B, Sequence alignment of TXR1 and its orthologues (accession numbers are provided in Table 3). Identical and similar amino acids are darkly and lightly shaded, respectively. The predicted Loop 3 (L3) in *Arabidopsis* ATXR5 was labeled with a blue box. Residues G363, Y364, E365, and E367 in Loop 3 are in red.

MATERIALS AND METHODS

Strains and culture

Cells of *Tetrahymena thermophila* were cultured in 1×SPP medium at 30°C with gentle shaking (Cassidy-Hanley et al., 1997). Log-phase cells (2×10^5 cells mL^{-1}) were used for phenotypic analyses. Cells were starved overnight in 10 mmol L^{-1} Tris (pH 7.4) before transformation by biolistic bombardment (Cassidy-Hanley et al., 1997). *HHT2*-WT (wild type) and *HHT2*-K27Q cells were as previously reported (Figure 2G) (Liu et al., 2004), in which the only macronucleus gene encoding a canonical H3 was either the wild-type *HHT2* or the one carrying K27Q mutation. *HHT2*-WT/*HHT3*-WT and *HHT2*-K27Q/*HHT3*-K27Q cells were as described below (Figure 2H).

HHT3-WT/Δ*HHT4*-chx and *HHT3*-K27Q/Δ*HHT4*-chx plasmid construction

Primers used for plasmid construction in this study are listed in Table 2.

HHT3 and *HHT4*, the two genes encoding the quantitatively minor histone H3 variants homologous to H3.3 in higher eukaryotes, are tandem arrayed in the *Tetrahymena* genome (Cui et al., 2006). For effective study of contributions from H3 variants, we have adopted a strategy to mutagenize one gene (*HHT3*) while deleting the other (*HHT4*). To generate *HHT3*-WT/Δ*HHT4-chx*, 5′ flanking region (~1 kb), CDS (441bp), and 3′ flanking region (~700 bp) of *HHT3* were amplified using primers HHT3_5f3206_Not I and HHT3_3r5337_neo. 3′ flanking region (~1 kb) of *HHT4*, ~230 bp away from the stop codon, was amplified using primers HHT4_3f15190_neo and HHT4_3r16252_Not I. The above-mentioned fragments, together with the *chx* cassette released from *pChx* vector by *Sma* I digestion (Gao et al., 2013), were assembled together by fusion PCR, and cloned into pBluescript SK (–) vector in *Not* I site. For *HHT3*-K27Q/Δ*HHT4*, a point mutation (K27Q) was introduced to *HHT3*, using primers HHT3_f4305_K27Q and HHT3_r4323_K27Q (Figure 2H and I).

Validation of complete somatic replacement by Quantitative-PCR (Q-PCR)

Q-PCR was performed in 96-well plate (Applied Biosystems, USA) with a total 25 μL of 12.5 μL SYBR Green PCR mix (Invitrogen, USA), 5 μL primers (forward and reverse, 1 μmol L^{-1}), and 7.5 μL whole cell lysate. Parameters for Q-PCR are: 50°C, 2 s; 95°C, 10 s; 40 cycles (95°C, 2 s; 50°C, 1 s; 60°C, 1 s), followed by a dissociation step. Primers matched to the CDS of *JMJ1* (TTHERM_00185640) are used as internal control (JMJ1_ f2071, JMJ1_r2236). Transformed cells with a normalized C_t difference more than 4 ($\Delta C_t \geq 4$; relative to WT cells) have achieved complete replacement in MAC (Table 1).

Immuno-fluoresence staining and imaging

Log-phase *Tetrahymena* cells (2×10^5 cells mL^{-1}) are labeled with BrdU for 30 min (0.4 mmol L^{-1}) in 1×SPP medium, and are fixed with 2% paraformaldehyde and permeabilized by

Table 2 Primers used in the present study[a)]

Primer name	Sequence (5′–3′)	Purpose
JMJ1_f2071	CTATCTAACGGAGTAATGTTTGCTG	For Q-PCR analysis as a loading control
JMJ1_r2236	AAGGTTGAGTGCATCCCATAACG	
HHT3_5f3206_Not I	*AGTTCTAGAGCGGCCGC*AATCTATTTATTACAAATGCATGTC*	To delete *HHT4* and mutate *HHT3* (K27Q)
HHT4_3r16252_Not I	*ACCGCGGTGGCGGCCGC*TTATTTTGTTTGTTTGTTTGGCG*	
HHT3_3r5337_neo	*GTCAGGTGCCTGGTACCC*GTGTATCTGTCTGTCTGGTTGTC*	
HHT4_3f15190_neo	*CTGACGTCGCACCATCCC*GATGCAAGTTATTTACTGTATTCCC*	
HHT3_f4305_K27Q	GCCAGAtAGTCTGCCCCCGTCTCTGGTGGTG**	
HHT3_r4323_K27Q	CGGGGGCAGACTaTCTGGCAGCCTTGGTAGCG**	
HHT3_3f5457	TACACATACTCATTCATGAGC	For Q-PCR analysis of *HHT2*-WT /*HHT3*-WT and *HHT2*-K27Q/*HHT3*-K27Q strains
HHT3_3r5623	GATTGTGAGCAATAACACG	

a) *, Characters in italics indicate adaptor sequences. **, Lowercase characters indicate mutations.

Table 3 Accession number of sequences used for alignment in Figure 4[a)]

	Protein name	Accession number
H3-H3.3 homologues	H3_Tet[1]	P69150
	H3.3_Tet[1]	P41353
	H3.1_Ara[2]	NP_201339.1
	H3.3_Ara[2]	NP_195713.1
TXR1 homologues	*Arabidopsis thaliana*_ATXR5	AAZ31374
	*Glycine max*_ATXR5	XP_003523236.1
	*Oryza sativa*_ATXR5	BAC05613.1
	*Arabidopsis thaliana*_ATXR6	NP_197821.1
	*Glycine max*_ATXR6	XP_003518664.1
	*Oryza sativa*_ATXR6	BAD07945.1
	*Physcomitrella patens*_TXR1	XP_001784397.1
	*Blastocystis hominis*_TXR1	CBK20503.2
	*Tetrahymena thermophila*_TXR1	XP_001019150
	*Paramecium tetraurelia*_TXR1	XP_001434344.1
	Paramecium tetraurelia-2_TXR1	XP_001430642.1
	*Ichthyophthirius multifiliis*_TXR1	EGR29795-6.1

a) Tet[1], *Tetrahymena thermophila*; **Ara[2], *Arabidopsis thaliana*.

adding 0.4% Triton X-100. The primary antibody is α-BrdU (Thermo Scientific, USA) and the secondary antibody is Alexa Fluor 488 goat anti-mouse IgG (Invitrogen). Samples were mounted with Prolong Gold antifade reagent with DAPI as a DNA-specific counterstain (Invitrogen). Digital images were collected using a Carl Zeiss Axio Imager Z1 microscope with a Carl Zeiss AxioCam HRc camera.

Sequence alignment

Amino acid sequences were aligned using MUSCLE (Edgar, 2004) with default parameters. Accession numbers were provided in Table 3.

Compliance and ethics *The author(s) declare that they have no conflict of interest.*

Acknowledgements *Our thanks are due to Prof. Weibo Song from Ocean University of China, for his kind help in preparing the draft and illustrations. We also thank Mr. Mingjian Liu, Lab. of Protozoology, Ocean University of China, for providing in vivo and protogal staining pictures of Tetrahymena. This work was supported by the Natural Science Foundation of China (31470064, 31522051 to Shan Gao), the National Institutes of Health (R01-GM087343 to Yifan Liu), AoShan Talents Program supported by Qingdao National Laboratory for Marine Science and Technology (2015ASTP), China and a research grant by Qingdao government (15-12-1-1-jch).*

Ahmad, K., and Henikoff, S. (2002). Epigenetic consequences of nucleosome dynamics. Cell 111, 281–284.
Allis, C.D., Glover, C.V.C., Bowen, J.K., and Gorovsky, M.A. (1980). Histone variants specific to the transcriptionally active, amitotically dividing macronucleus of the unicellular eucaryote, *Tetrahymena thermophila*. Cell 20, 609–617.
Bannon, G.A., Calzone, F.J., Bowen, J.K., Allis, C.D., and Gorovsky, M.A. (1983). Multiple, independently regulated, polyadenylated messages for histone H3 and H4 in *Tetrahymena*. Nucleic Acids Res 11, 3903–3917.
Beh, L.Y., Müller, M.M., Muir, T.W., Kaplan, N., and Landweber, L.F. (2015). DNA-guided establishment of nucleosome patterns within coding regions of a eukaryotic genome. Genome Res 25, 1727–1738.
Berger, S.L. (2002). Histone modifications in transcriptional regulation. Curr Opin Genet Dev 12, 142–148.

Burman, B., Zhang, Z.Z., Pegoraro, G., Lieb, J.D., and Misteli, T. (2015). Histone modifications predispose genome regions to breakage and translocation. Genes Dev 29, 1393–1402.
Cassidy-Hanley, D., Bowen, J., Lee, J.H., Cole, E., VerPlank, L.A., Gaertig, J., Gorovsky, M.A., and Bruns, P.J. (1997). Germline and somatic transformation of mating *Tetrahymena thermophila* by particle bombardment. Genetics 146, 135–147..
Chen, X., Gao, S., Liu, Y., Wang, Y., Wang, Y., and Song, W. (2016). Enzymatic and chemical mapping of nucleosome distribution in purified micro- and macronuclei of the ciliated model organism, *Tetrahymena thermophila*. Sci China Life Sci doi: 101007/s11427-016-0137-3.
Cole, E., and Sugai, T. (2012). Developmental progression of *Tetrahymena* through the cell cycle and conjugation. Methods Cell Biol 109, 177–236..
Cui, B., Liu, Y., and Gorovsky, M.A. (2006). Deposition and function of histone H3 variants in *Tetrahymena thermophila*. Mol Cell Biol 26, 7719–7730.
Edgar, R.C. (2004). MUSCLE: multiple sequence alignment with high accuracy and high throughput. Nucleic Acids Res 32, 1792–1797.
Engelen, E., Brandsma, J.H., Moen, M.J., Signorile, L., Dekkers, D.H., Demmers, J., Kockx, C.E., Ozgür, Z., van IJcken, W.F., and van den Berg, D.L. (2015). Proteins that bind regulatory regions identified by histone modification chromatin immunoprecipitations and mass spectrometry. Nat Commun 6, 7115.
Felsenfeld, G., and Groudine, M. (2003). Controlling the double helix. Nature 421, 448–453.
Gao, F., Warren, A., Zhang, Q., Gong, J., Miao, M., Sun, P., Xu, D., Huang, J., Yi, Z., and Song, W. (2016). The all-data-based evolutionary hypothesis of ciliated protists with a revised classification of the Phylum Ciliophora (Eukaryota, Alveolata). Sci Rep 6, 24874.
Gao, S., Xiong, J., Zhang, C., Berquist, B.R., Yang, R., Zhao, M., Molascon, A.J., Kwiatkowski, S.Y., Yuan, D., Qin, Z., Wen, J., Kapler, G.M., Andrews, P.C., Miao, W., and Liu, Y. (2013). Impaired replication elongation in *Tetrahymena* mutants deficient in histone H3 Lys 27 monomethylation. Genes Dev 27, 1662–1679.
Iizuka, M., and Smith, M.M. (2003). Functional consequences of histone modifications. Curr Opin Genets Dev 13, 154–160.
Jacob, Y., Bergamin, E., Donoghue, M.T.A., Mongeon, V., LeBlanc, C., Voigt, P., Underwood, C.J., Brunzelle, J.S., Michaels, S.D., Reinberg, D., Couture, J.F., and Martienssen, R.A. (2014). Selective methylation of histone H3 variant H3.1 regulates heterochromatin replication. Science 343, 1249–1253.
Jacob, Y., Feng, S., LeBlanc, C.A., Bernatavichute, Y.V., Stroud, H., Cokus, S., Johnson, L.M., Pellegrini, M., Jacobsen, S.E., and Michaels, S.D. (2009). ATXR5 and ATXR6 are H3K27 monomethyltransferases required for chromatin structure and gene silencing. Nat Struct Mol Biol 16, 763–768.
Jacob, Y., Stroud, H., LeBlanc, C., Feng, S., Zhuo, L., Caro, E., Hassel, C., Gutierrez, C., Michaels, S.D., and Jacobsen, S.E. (2010). Regulation of heterochromatic DNA replication by histone H3 lysine 27 methyltransferases. Nature 466, 987–991.
Karrer, K.M., and VanNuland, T.A. (2002). Methylation of adenine in the nuclear DNA of *Tetrahymena* is internucleosomal and independent of histone H1. Nucleic Acids Res 30, 1364–1370.
Kornberg, R.D., and Thonmas, J.O. (1974). Chromatin structure: oligomers of the histones. Science 184, 865–868.
Liu, M., Fan, X., Gao, F., Gao, S., Yu, Y., Warren, A., and Huang, J. (, and 2016). *Tetrahymena australis* (Protozoa, Ciliophora): a well-known but "non-existing" taxon—consideration of its identification, definition and systematic position. J Eukaryot Microbiol doi: 10.1111/jeu.12323.
Liu, Y., Mochizuki, K., and Gorovsky, M.A. (2004). Histone H3 lysine 9 methylation is required for DNA elimination in developing macronuclei in *Tetrahymena*. Proc Natl Acad Sci USA 101, 1679–1684.
Meyer, E., and Chalker, D.L. (2007). In: Epigenetics, C.D. Allis, M.L. Caparros, T. Jenuwein and D. Reinberg, eds. (Cold Spring Harbor, New York) pp. 127–150.
Ray-Gallet, D., Quivy, J.P., Scamps, C., Martini, E.M.D., Lipinski, M., and Almouzni, G. (2002). HIRA is critical for a nucleosome assembly pathway independent of DNA synthesis. Mol Cell 9, 1091–1100.
Strahl, B.D., and Allis, C.D. (2000). The language of covalent histone modifications. Nature 403, 41–45.
Tagami, H., Ray-Gallet, D., Almouzni, G., and Nakatani, Y. (2004). Histone H3.1 and H3.3 complexes mediate nucleosome assembly pathways dependent or independent of DNA synthesis. Cell 116, 51–61.
Thatcher, T.H., and Gorovsky, M.A. (1994). Phylogenetic analysis of the core histones H2A, H2B, H3, and H4. Nucleic Acids Res 22, 174–179.
Thatcher, T.H., MacGaffey, J., Bowen, J., Horowitz, S., Shapiro, D.L., and Gorovsky, M.A. (1994). Independent evolutionary origin of histone H3.3-like variants of animals and *Tetrahymena*. Nucleic Acids Res 22, 180–186.
Woodard, J., Kaneshiro, E., and Gorovsky, M.A. (1972). Cytochemical studies on the problem of macronuclear subnuclei in *Tetrahymena*. Genetics 70, 251.
Zhang, C., Gao, S., Molascon, A.J., Liu, Y., and Andrews, P.C. (2014). Quantitative proteomics reveals histone modifications in crosstalk with H3 lysine 27 methylation. Mol Cell Proteomics 13, 749–759.
Zhang, C., Molascon, A.J., Gao, S., Liu, Y., and Andrews, P.C. (2013). Quantitative proteomics reveals that the specific methyltransferases Txr1p and Ezl2p differentially affect the mono-, di- and trimethylation states of histone H3 lysine 27 (H3K27). Mol Cell Proteomics 12, 1678–1688.